

INVESTIGATION ON OPTICAL AND ELECTRICAL PROPERTIES OF LPCVD SiO_xN_y THIN FILMS

M. Modreanu¹, Mariuca Gartner², A. Szekeres³, S. Alexandrova³

¹National Institute for R&D in Microtechnologies PO Box 38-160, Bucharest 72225 Romania; E-mail: mirceam@imt.ro

²Institute of Physical Chemistry, Spl.Independentei 202, Bucharest 77208, Romania

³Institute of Solid State Physics, Tzarigradsko Chaussee 72, Sofia 1784, Bulgaria

ABSTRACT

Amorphous silicon oxynitride ($a\text{-SiO}_x\text{N}_y$) films of various compositions were deposited by low-pressure chemical vapour deposition (LPCVD) at temperature range of 820-880°C and 400 mTorr, using mixture of $\text{SiCl}_2\text{H}_2\text{-NH}_3\text{-N}_2\text{O}$. The investigation on optical and electrical properties was made using spectroellipsometry (SE) and the analyses of 1 MHz capacitance-voltage characteristics. To calculate optical and microstructural parameters of the films we used different approaches (Bruggeman-EMA, Cauchy, Sellmeier and Wemple-Di Domenico). The observed low densities of the interface traps are attributed to the nitrogen incorporation at the $\text{SiO}_x\text{N}_y/\text{Si}$ interface which leads to suppression of their generation.

1. INTRODUCTION

The low pressure chemical vapour deposition (LPCVD) silicon oxynitride (SiO_xN_y) films have several applications in microelectronics and optoelectronics industry: passivating coatings [1-6], thin gate dielectrics [2] and, membranes and optical wave guides for microelectro-mechanical systems (MEMS) [3]. Controllable variable refractive index of the silicon oxynitride films, which are of growing interest in integrated opto-electronical devices, resistance to oxidation, low mechanical stress are some properties of these films.

This paper presents the correlation between deposition parameters, material properties and internal structure. The investigation on optical and electrical properties was made using spectroellipsometry (SE) and the analyses of 1 MHz capacitance-voltage characteristics. In order to calculate the optical and microstructural properties of the films from spectro-ellipsometric data, we used three different approaches: Bruggeman-EMA[7] Cauchy and Sellmeier [8].

2. EXPERIMENTAL DETAILS

LPCVD silicon oxynitride thin films were deposited on 3-inch (100) p-type silicon wafers. The $a\text{-SiO}_x\text{N}_y$ films were formed by reacting dichlorosilane (SiH_2Cl_2) with nitrous oxide (N_2O) and ammonia (NH_3). The total deposition pressure was 400 mTorr. Relative gas flow ratio $r = Q_{\text{N}_2\text{O}}/Q_{\text{NH}_3}$, deposition temperature and pressure have a great influence on the film composition. Two of these parameters were varied during our experiments: the relative gas flow ratio was between 0 and 8 for 860°C deposition temperature; keeping the r parameter constant ($r=3.5$) the deposition temperature was increased from 820°C to 880°C. We have also deposited the silicon nitride films from dichlorosilane and ammonia (NH_3) at 800°C using a relative gas flow ratio $\text{SiH}_2\text{Cl}_2/\text{NH}_3 = 0.25$. Before deposition, the substrates were chemically cleaned using a 10 % HF solution in order to remove the native oxide.

The film thickness, the dispersion of the refractive index and optical gap were determined using spectroscopic ellipsometry in 320 - 800nm wavelength range. All SE measurements were done at an incidence angle of 70°.

For electrical characterization of LPCVD- SiO_xN_y films, conventional, room temperature 1 MHz C-V technique was applied. For this purpose, metal-insulator-silicon (MIS) capacitors were formed by vacuum thermal evaporation of aluminum dots onto SiO_xN_y surface through a metal mask, while onto silicon backside continuous Al film was evaporated. The effective dielectric charge density (Q_{eff}) was calculated from the flat band voltage shift in the 1 MHz C-V curves. The interface traps density (D_{it}) was estimated from the comparison of the 1 MHz experimental and corresponding ideal C-V characteristics.

3. RESULTS AND DISCUSSIONS

The most significant optical properties in amorphous materials, the optical gap (E_g) and the refractive index (n) could be obtained using the SE measurements. Normally, both of them depend on the composition of the films. We have calculated the coefficients x and y in the SiO_xN_y formula using Temple-Boyer formula (error lower than 1%) [9]:

$$n = 2 - 0.4x + 0.07x^2 = 1.45 + 0.19y + 0.16y^2 \quad (1)$$

and the results are given in **Table 1**. The sample identification is made by its refractive index values (at $\lambda = 632.8$ nm). In the last row of the table 1 there are the values for Si_3N_4 and we can observe that the normalization to the silicon label produces the good value for nitrogen.

TABLE 1: Results concerning the film composition, obtained using the Temple-Boyer formula

n	x	y
1.61	1.21	0.56
1.70	0.86	0.79
1.82	0.50	1.04
1.98	0.05	1.32
2.00	0	1.34

We have studied the spectral dispersion of the refractive index for our five different $\text{a-SiO}_x\text{N}_y$ samples (Fig.1). The dispersion spectra of the refractive index was fit using the Cauchy formula: $n = \alpha + \frac{\beta}{\lambda^2}$ (2), where α and β are the Cauchy's parameters and λ is the wavelength of light used at SE. For $\lambda \rightarrow \infty$, the significance of the α parameter appears immediately as n_∞ . The values of the fit parameters and the fit quality parameter (χ^2) are presented in **Table 2**.

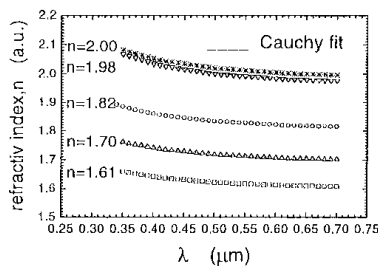


Fig 1 The refractive index dispersion and the fit with Cauchy's formula

TABLE 2. Cauchy parameters and the fit quality

n	α	β ($\cdot 10^{-2}$)	χ^2
1.61	1.59	0.87	$1.3 \cdot 10^{-6}$
1.70	1.68	0.90	$6.3 \cdot 10^{-7}$
1.82	1.78	0.11	$1.25 \cdot 10^{-6}$
1.98	1.94	1.5	$2.39 \cdot 10^{-6}$
2.00	1.97	1.3	$1.22 \cdot 10^{-6}$

Another model used in the refractive index dispersion study is the Sellmeier' model that

$$\text{gives: } n^2 = 1 + \frac{A\lambda^2}{\lambda^2 - B} \quad (3), \text{ where A and B are}$$

the Sellmeier parameters. Under these conditions we can see that $n_\infty = \sqrt{1+A}$ and the calculated values are given in the fourth column of the **Table 3**. Comparing these values with the α values from table 2 we find a very good agreement.

TABLE 3. Sellmeier constants for the studied SiO_xN_y thin films

n	A	$B \cdot 10^{-2}$	n_∞	$B \cdot 10^{-2}$ (eqn (5))
1.61	1.8263	1.5794	1.59	1.512
1.7	1.8476	1.5653	1.68	1.564
1.82	2.221	1.614	1.79	1.610
1.98	2.792	1.787	1.85	1.784
2.00	2.882	1.646	1.97	1.644

Wemple and Di Domenico [10] have developed a model where the refractive index dispersion is studied in the region of transparency, below the gap, using the single-oscillator approximation. Defining two parameters, the oscillation energy, E_0 , and the dispersion energy, E_d , the model concludes:

$$n^2(\omega) - 1 \cong \frac{E_d E_0}{E_0^2 - E^2} \quad (4)$$

Both Wemple parameters can be obtained from the slope and the intercept with Y axis of the plot $(n^2 - 1)^{-1} = f(E^2)$. The energy oscillation and dispersion energy values are given in **Table 4**. The dispersion energy measures the average strength of interband optical transitions. Wemple and Di Domenico have related this parameter with the coordination number for anion and the valence electrons number per anion. In our case the E_d values increase with increasing the silicon nitride relative percentage in the films (the bonds' number per nitrogen atom is higher in comparison with that of oxygen atom). The oscillator energy is related by an empirical formula to optical gap value:

$E_0=1.7E_g$ [11,12] The calculated values of the optical gap are also presented in table 4. We can see that, higher oxygen content in film means a higher optical gap value. This result is very important because it shows that the refractive index and the optical gap of the material can be controlled by the deposition conditions.

Applying the Sellmeier's model and the Wemple's model on the same photon energy range, the A and B parameters can be expressed as:

$$A = \frac{E_d}{E_0} \text{ and } B = \frac{h^2 c^2}{E_0^2} \quad (5), \text{ where } h \text{ is the}$$

Plank's constant and c is the light speed in vacuum.

We have calculated the B-parameter values using eqn (5) and the results are given in **Table 3**. A comparison between the third and the fifth columns shows the good agreement between the two optical models.

TABLE 4. Optical gap and Wemple Di Domenico parameters for the studied films

n	E_d (eV)	E_0 (eV)	E_g (eV)
1.61	15.48	10.09	5.93
1.73	18.25	9.96	5.86
1.82	21.66	9.78	5.75
1.98	25.94	9.28	5.46
2.00	27.87	9.23	5.43

The influence of the relative percentage of oxygen on the optical gap values can be observed from the correlation of the results presented in **Table 1** and **4**. In such way, we have correlated the two optical films' parameters between them and, an optical one with a structure parameter. As it is known, when the effective refractive index decreases, the value of the optical gap increases. One the other hand, higher silicon dioxide in the film means higher optical gap values. For silicon nitride film, we have obtained a good agreement with the literature, concerning the optical gap : 5.43eV in comparison with 5.35 eV [13].

Typical high-frequency capacitance curves for $\text{SiO}_{0.50}\text{N}_{1.04}$ and $\text{SiO}_{0.86}\text{N}_{0.79}$ samples are plotted in Fig. 2. The density of effective fixed oxide charge Q_{eff} as estimated from the flatband voltage shifts are estimated from the flatband voltage values and are presented in Table 5. For sample

$\text{SiO}_{0.50}\text{N}_{1.04}$ no hysteresis in the C-V curve and lower Q_{eff} are observed. This can be related to higher amount of nitrogen present in the near-interface region, which attaches unsaturated Si bonds ($\text{O}_3\equiv\text{Si}^{\cdot}$) being responsible for the fixed oxide charge defect states. As the oxygen content increases, the interface region approaches the standard Si/SiO₂, as can be seen in Fig.1. The small hysteresis is indicative for the presence of slow interface traps with a density of $4 \times 10^{10} \text{ cm}^{-2}$.

The densities of the interface traps are displayed in Fig. 3, given in Table 5. The dielectric permittivity, ϵ_i , is calculated from the dielectric capacitance, C_i , in the strong accumulation regime ($C_i = \epsilon_i \epsilon_0 s / t_i$). Its value is also given in Table 5. According to the refractive index behavior, as the oxide fraction becomes higher in the film structure the dielectric permittivity decreases.

TABLE 5 The dopant density, N_a , the effective dielectric charge density, Q_{eff} , and the dielectric permittivity, ϵ_i for $\text{SiO}_{0.50}\text{N}_{1.04}$ (1) and $\text{SiO}_{0.86}\text{N}_{0.79}$ (2) samples

Sample	N_a (cm ⁻³)	Q_{eff} (cm ⁻²)	ϵ_i
1	1.3×10^{15}	1.42×10^{11}	5.10
2	1.3×10^{15}	3.82×10^{11}	4.42

The distribution of the interface traps over the silicon energy gap is displayed in Fig. 3. Again, the higher nitrogen content leads to smaller density over most of the bandgap. Obviously, trivalent Si such as $\text{Si}_3\equiv\text{Si}^{\cdot}$ forms rigid Si-N bonds reducing the intrinsic stress at the interface.

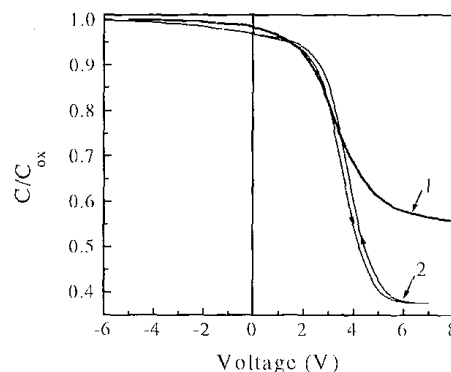


Fig. 2 Normalized 1 MHz capacitance-voltage characteristics of MIS structures for $\text{SiO}_{0.50}\text{N}_{1.04}$ (1) and $\text{SiO}_{0.86}\text{N}_{0.79}$ (2) sample

As a consequence, the density of interface traps related to dangling and deformed bonds becomes lower. The lower intrinsic stress at the interface is supported by the low trap density approaching the conduction band edges.

The higher density near midgap, in the sample with deficit in nitrogen, can be connected with large amount of trivalent Si defect centers.

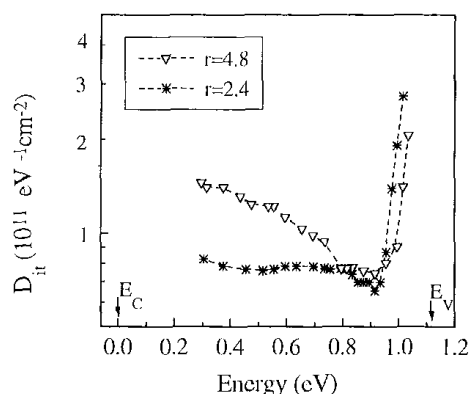


Fig. 3 Energy distribution of interface traps, D_{it} , in the Si forbidden band gap

4. CONCLUSION

The summary of this paper can be synthesized as:

- Deposition of LPCVD a-SiON films it's a good solution to obtain films with controlled refractive index
1. The dispersion of the refractive index for samples with different silicon dioxide content was successfully fitted with Cauchy and Sellmeier formula
 2. The optical gap energy (E_g) and the oscillator energy (E_0) become higher, while the oscillator strength (E_d) lower, with increase of the silicon dioxide in the film. The latter is indicative for the stronger Si-N than Si-O bonds.
 3. The optical gap and the dispersion energy values were determined using Wemple and Di Domenico approximation.

From the C-V data analysis we can conclude that the observed much lower total density of defects in SiO_xN_y in comparison with conventional thermal SiO_2/Si structures is due to the effect of incorporation of nitrogen, which produces strong S-N bonds to replace the weak Si-O bonds and to saturate the dangling $\text{O}_\beta\text{-Si}^\cdot$ and $\text{Si}_\beta\text{-Si}^\cdot$ bonds.

REFERENCES

1. A.J. Lowe, M.J. Powell and S.R. Elliott. *J. Appl. Phys.* **59** (1986) 1251.
2. B.B. Ilic, *Hewlett Packard J.* **33** (1982) 25
3. M. Modreanu, P. Cosmin, *Procc. of Int. Conf. of Semic.-CAS'96* (1996), 323
4. H. Kurata, M. Hirose and Y. Osaka, *Jap. J. of Appl. Phys.* **20**, No. 11 (1981) L811
5. F.H.P.M. Habraken, R.H.G. Tijhaar, V.F van der Weg, A.E.T. Kuiper and M.F.C. Willemsen, *J. of Appl. Phys.* **59** (1986), 447
6. B.H. Augustine, E.A. Irene, Y.J. He, K.J. Price, L.E. McNeil, K.N. Christensen and D.M. Maher, *J. of Appl. Phys.* **78** (1995), 402
7. D.A.G. Bruggeman, *Ann. Phys.* **24** (1935), 636
8. M. Born and E. Wolf, *Principles of Optics*, Pergamon Press, Oxford (1975), Chapter II.
9. P. Temple-Boyer, B. Hajji, J.L. Alay, J.R. Morante, A. Martinez, E' MRS'99, Book of abstracts
10. S.H. Wemple and M. DiDomenico, *Phys. Rev. B* vol. **3**, nr.4 (1971), 1338
11. N. Tomozeiu, *PhD Theses*, Bucharest University, (1994)
12. I. Solomon, M.P. Schmidt, C. S enemaud, and M. Driss Khodja, *Phys. Rev. B* **38**, nr.18 (1988), 13263
13. A. Borghesi, A. Sassela, S. Rojas, *Thin Solid films*, **233** (1993), 227